Flexible support structure design for optical mirror

Ning Xu [a,b,*], FuSheng Zhang [a,b], AnBo Jiang [a]

[a] *Changshu Institute of Technology, Changshu, 215500, China*
[b] *Key Construction Laboratory for Elevator Intelligent Safety in Jiangsu Province (Changshu Institute of Technology), Changshu, 215500, China*

A B S T R A C T

In order to realize the high-precision assembly of the mirror of the aeronautical optical system, a semi-kinematic flexible support structure applied to the airborne field was designed. This paper studies the support principle and assembly method of flexible support of mirror. Firstly, according to the kinematic theory of space mechanism, the spatial degrees of freedom of the mirror were theoretically analyzed. Then, in view of the difficulties encountered in the assembly and application of the mirror, a flexible support structure was designed. Then, the design results were verified by means of finite element analysis. Finally, the processing and assembly of a flexible support structure of the mirror was completed, and the relevant experimental tests were carried out. The experimental results show that the accuracy of the mirror after assembly with flexible support structure is better than $\lambda/50$ ($\lambda = 632.8$ nm), and the mass is less than 2 kg. The model fundamental frequency modal of the whole assembly is 645 Hz, which is higher than the design requirement. All simulation and test results show that the flexible support structure works well, meets the requirements of aviation optical system, and has the advantages of simple assembly, high precision, stability and reliability.

1. Introduction

Optical imaging payloads play an important role in areas such as national production, astronomical exploration, and earth sciences [1–7]. The advantages and disadvantages of the mirror support structure in the optical imaging payload will directly affect accuracy of the mirror, thereby affecting the imaging quality of the entire optical system. Due to the large weight and size of some mirrors, it is difficult to mount such mirrors. Typical problems are [8–12]:

- **Bonding stress**: Non-metallic mirrors (glass or ceramic) require the use of adhesives, which are bonded to the bushings to facilitate connection with the support structure, and during the curing of the adhesive, adhesive stresses are generated between the mirrors and the bushings.
- **Assembly stress**: When the back plate of the mirror is connected to the mirror through a flex joint, the two mounting planes have residual processing errors and assembly errors, and the screws will generate assembly stress between the back plate and the flexible joint during the process of applying pretension.

- **Temperature stress**: Generally, the mirror and the support structure are processed from different materials, and when the surrounding temperature changes, the thermal expansion of the mirror and the support structure will cause temperature stress between the installation interface.

All three stresses cause the optical surface to be misaligned or deformed. Most of the existing mirror mounting structures are over-constrained systems, and excessive constraints cannot eliminate assembly stress and temperature stress, which will cause the offset of the mirror position and the deformation of the surface of the mirror, thereby degrading the imaging quality of the entire optical system. Therefore, this paper aims to design a flexible support structure of optical mirror to eliminate the above stress, ensure the position accuracy and surface accuracy of the mirror, and improve the imaging quality of the optical system. The support structure can be applied to aerial reconnaissance, security monitoring, natural resource investigation, helicopter search and rescue, etc.

2. Flexible support principle

2.1. Mirror support principle

According to the theory of mechanism, unconstrained optical mirrors have six spatial degrees of freedom as shown in Fig. 1 [13]. These are the degrees of translation freedom along three axes: TX, TY, TZ, and the degrees of rotation around the three axes: RX, RY, RZ. The mirror support structure must achieve complete constraints on these six degrees of freedom, and both under-constrained and over-constrained will have serious consequences. If the mirror is under-constrained, its unconstrained degrees of freedom will produce uncontrollable random motion, and the position of the mirror is not fixed. If the mirror is over-constrained, the excess constraint will create stress in the mirror body, further affecting the accuracy of the mirror.

After the above analysis, it can be concluded that the principles of the optical mirror support structure design are:

- All degrees of freedom of the mirror are fully constrained;
- During assembly and application, mirror shape errors and rigid body displacements are kept as small as possible;
- The fundamental frequency of the support structure components meets the requirements of the system.

2.2. Flexible support principle

The support structure of large optical mirrors mainly includes rigid support and flexible support. The rigid support uses joint mechanisms such as ball bearings or hinges to release its excess degrees of freedom to achieve the purpose of fully constraining the six degrees of freedom of the mirror. Rigid support due to the gap of the joint mechanism, which can produce friction, wear, and even collision impact in dynamic load applications, therefore, more and more optical mirrors are supported by flexible structures [14–20].

The flexible support structure of the optical mirror, which sets flexible units of different shapes at its key positions, uses the slight deformation of the material to achieve the release of degrees of freedom, thereby replacing the rigid joint mechanism. Compared with rigid support structure, flexible support structure has the advantages of no gap, no friction and no wear.

The schematic of the flexible support structure of the optical mirror designed in this paper is shown in Fig. 2. Three identical composite flexible supports are installed on the back of the mirror, and the three flexible supports are evenly distributed 120° apart. Each composite flexible support is designed with multiple flexible hinges to achieve the release of four spatial degrees of freedom,
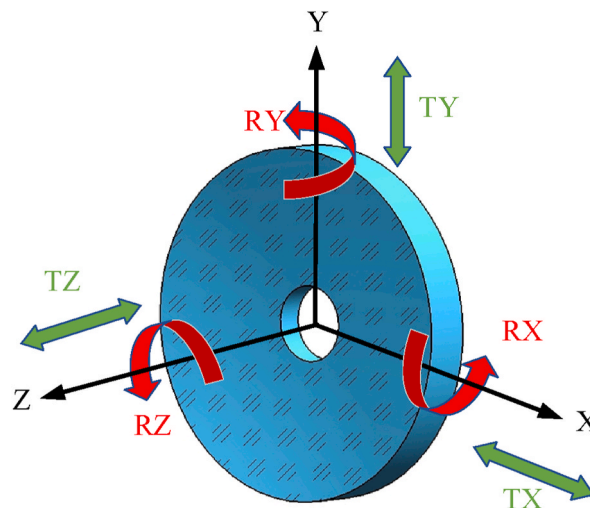

Fig. 1. Schematic diagram of the spatial degrees of freedom of an optical mirror.
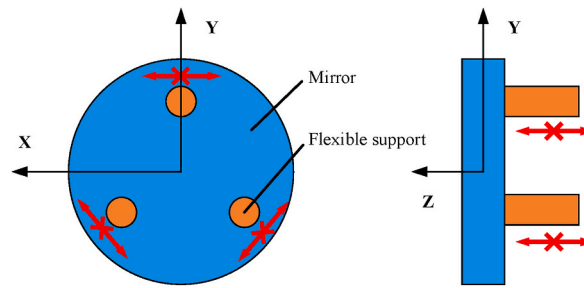
Fig. 2. Flexible support schematic of optical mirror.

which are three rotational degrees of freedom and one transnational freedom. The remaining two rigid support directions are axial and transverse along the flexible support. The axial stiffness constraint direction of the flexible support is consistent with the axial direction of the mirror, and the lateral stiffness constraint direction of the flexible support is arranged along the tangential direction of the optical mirror, as shown in Fig. 2.

Three rigid constraints along the tangential direction of the optical mirror constrain the mirror's three degrees of freedom: TX, TY and RZ. Three rigid constraints along the optical mirror's optical axis constrain the mirror's three degrees of freedom: TZ, RX and RY. As a result, this flexible support structure achieves fully constraint of the optical mirror. This flexible support structure has the following advantages:

- **Absorbing installation stress**: Due to the accumulation of errors in the processing and assembly process, there will be a height error or (and) angle error between the three flexible supports, when it is installed on the back plate, because each flexible support has a corresponding flexibility, it can absorb a part of the installation stress and reduce the mirror deformation error caused by the installation stress;
- **Absorbing temperature stresses**: Due to the inconsistency between the mirror and the supporting structural material, there is a difference in the coefficient of linear expansion. Therefore, when the ambient temperature changes, the different thermal expansions of the mirror and the support structure create temperature stress between the mounting interfaces. Since the flexible support structure designed in this paper is flexible in the radial direction of the mirror, it can absorb the structural stress caused by its temperature change and reduce the mirror error.

3. Mirror flexible support structure design

3.1. Design requirements

The mirror designed in this paper is the primary mirror in Cassegrain's optical system, made of silicon carbide and has a lightweight back. The mirror diameter is 232 mm, the mass is 852 g, and the weight reduction rate is 72.5%. The mirror is used in aeronautical optical systems, and the design of mirror components should comprehensively consider the influence of static load, dynamic load and ambient temperature.
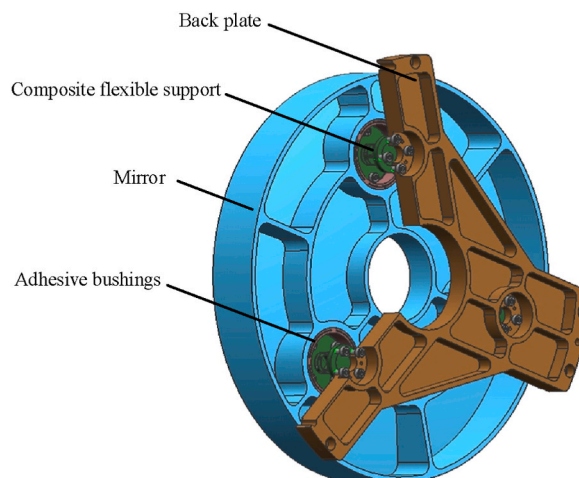

Fig. 3. Diagram of the flexible support structure of the mirror.

The requirements are as follows:

- The accuracy (rms) of the mirror component is better than λ/50 (λ = 632.8 nm);
- Under gravity load, the rigid body displacement of the mirror is less than 0.01 mm, and the inclination angle is less than 2″;
- The mass of the mirror assembly is less than 2 kg;
- The fundamental frequency of the mirror assembly is higher than 150 Hz.

3.2. Structure of the mirror assembly

The structure of the mirror assembly designed in this paper is shown in Fig. 3.

The back of the mirror is machined with three evenly distributed mounting holes. The three adhesive bushings are bonded together with the mirror by optical epoxy adhesive, and the material is Invar, whose expansion coefficient is consistent with that of the silicon carbide, eliminating the temperature stress caused by the ambient temperature change.

The lower mounting flange of the composite flexible supports is connected to the adhesive bushing by screws, and passes through the plane of the center of mass of the mirror to eliminate the gravitational inclination of the mirror caused by mass imbalance. The back plate is connected to the upper mounting flange of the composite flexible support by screws. The composite flexible support and back plate are made of titanium alloy material with low density, high strength and fatigue resistance.

3.3. Design of adhesive bushings

In order to eliminate the mirror stress introduced by the adhesive curing shrinkage, the adhesive bushing designed in this paper is shown in Fig. 4.

The outer cylinder of the adhesive bushing is machined with multiple penetration slits, with openings cut in the middle of each through slit, and the inner bottom surface is machined with mounting planes and mounting threaded holes for the installation of composite flexible supports. The penetrating slits are evenly distributed on the outer cylinder of the adhesive bushing, and the number of them is preferably greater than or equal to three, while the adhesive bushing designed in this paper has four penetrating slits. The epoxy adhesive is evenly applied to the outer surface of the cylinder of the adhesive bushing and the inner surface of the mirror mounting hole. During the curing process, epoxy adhesive will produce shrinkage stress between the inner surface of the mounting hole of the mirror and the outer surface of the bonding bushing cylinder, and the penetration slit will produce a small elastic deformation under the action of shrinkage stress, thereby reducing the tensile stress on the mirror and maintaining the accuracy of the mirror. The width of the incision in the middle of each penetration slit is very small, and it is processed by the EDM method, retaining most of the outer cylindrical surface (i.e., bonding area), and has high bonding strength.

3.4. Design of composite flexible supports

The composite flexible support is the key element of the mirror support structure, and its structure is shown in Fig. 5.
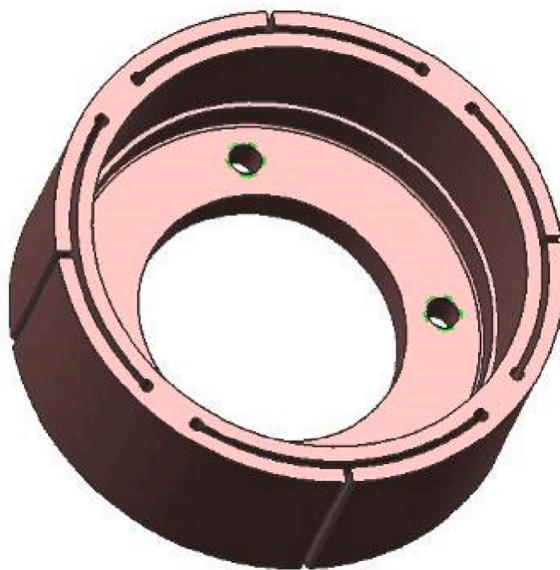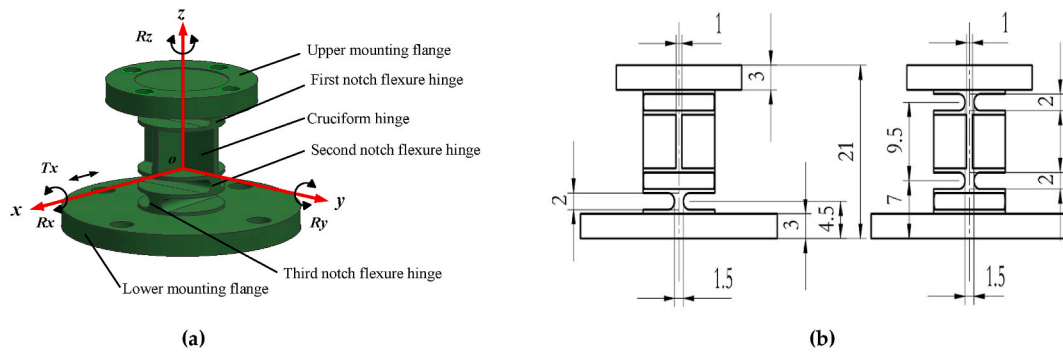

**Fig. 4.** Diagram of the adhesive bushing.

Fig. 5. Diagram of composite flexible support: (a) Outline drawing; (b) Dimensions. Fig. 5 shows the composite flexible support structure and the local coordinate definition diagram, and its local coordinate system is represented by the lowercase letter xyz to distinguish it from the mirror assembly coordinate system XYZ. The composite flexible support consists of upper mounting flange, first notch flexible hinge, cruciform hinge, second notch flexible hinge, third notch flexible hinge and lower mounting flange.

The upper mounting flange is used to connect the composite flexible support with the back plate, and the lower mounting flange is used to connect the composite flexible support to the adhesive bushing. The incision direction of the first notch flexible hinge and the second notch flexible hinge is parallel to the y-axis, and has the degree of freedom to rotate around the y-axis, and the combined movement of these two incision-types flexible hinges can produce flexible translational motion along the x-axis. The cruciform flexible hinge is machined along the z-axis and have degrees of freedom to rotate around the z-axis. The incision direction of the third notch flexible hinge is parallel to the x-axis, and it has the degree of freedom to rotate around the x-axis. Based on the above analysis, the composite flexible support can produce a flexible translation motion Tx in one direction and a flexible rotational motion Rx, Ry and Rz in three directions, limiting the translation motion Tz along the z-axis and the translation motion Ty along the y-axis.

The three composite flexible supports are evenly arranged along the same circumference, with the x-axis direction following the radial direction of the mirror, as shown in Fig. 2. Since the composite flexible support limits the translational motion Tz along the x-axis, the combination of the three composite flexible supports limits the rotational motion of the mirror along the X-axis, the rotational motion along the Y-axis, and the translational motion along the Z-axis. Since the composite flexible support limits the translational motion Ty along the y-axis, the combination of the three composite flexible supports limits the translational motion along the X-axis, the translational motion along the Y-axis, and the rotational motion along the Z-axis of the mirror. The six spatial degrees of freedom of the mirror are constrained, indicating that the flexible support structure is a fully constraint structure.

When the temperature changes, due to the inconsistency between the mirror and the back plate material, the mirror and the back plate have a relative motion trend in the radial direction. Since the three composite flexible supports have translational degrees of freedom along the x-axis, and this direction is arranged in the radial direction of the mirror, the flexible support structure is able to generate flexible micro-motion in the radial direction, thereby eliminating temperature stress. When the mounting flange plane of one
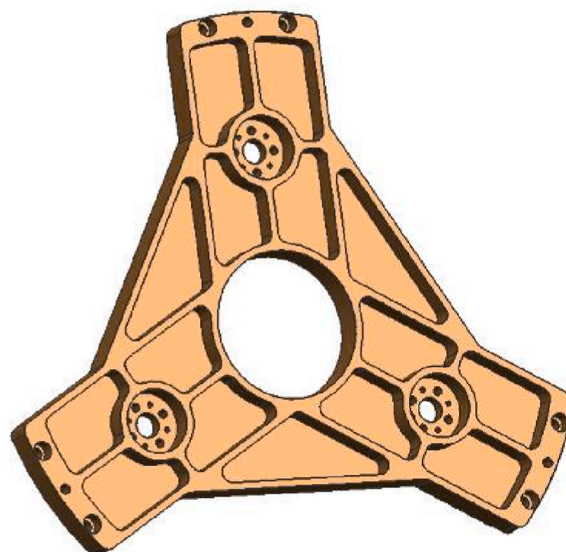
Fig. 6. Diagram of the back plate.

composite flexible support is not co-planar with the mounting flange plane of the other two composite flexible supports due to processing or assembly error, meanwhile the three composite flexible supports are installed together with the back plate, the mirror will produce a rotational movement tendency. Since the composite flexible support has the degree of freedom of rotation, the flexible support structure is able to generate a rotating flexible micro-movement, thereby eliminating assembly stress.

The composite flexible hinge is made of titanium alloy material, which machining method is wire cutting. The dimensional drawing conforming to the flexible hinge is shown in Fig. 5b. The hinge cutout is circular and has a diameter of 2 mm. The width of the cruciform flexible hinge is 1 mm.

3.5. Design of the back plate

The back plate is the main load-bearing structure of the mirror assembly, which is used to install the assembled mirror assembly into the optical system, and the back plate is also the assembly standard of the mirror assembly, which requires good rigidity, light weight and good dimensional stability. The triangular back plate structure designed in this paper is shown in Fig. 6, using titanium alloy material, with a mass of about 0.67 kg. The estimated mass of the model of the entire assembly is 1.7 kg, which is less than 2 kg.

4. Simulation analysis

According to the requirements of the mirror assembly, the static and dynamic simulation of the mirror assembly was carried out. The finite element model of the mirror assembly is shown in Fig. 7.

4.1. Static analysis

Since the aeronautical optical payload will experience large-angle scanning motion and aircraft maneuvering action during application, the static features of the mirror assembly in all directions should be analyzed. Gravity loads are applied in the X direction (horizontal optical axis) and Z direction (vertical optical axis) to analyze the surface accuracy and rigid body displacement of the entire assembly under various working conditions. The deformation contour plot of the mirror assembly under gravity load in the X direction is shown in Fig. 8a. The deformation contour plot of the mirror assembly under gravity load in the Z direction is shown in Fig. 8b.

The mirror node data were extracted, and the surface shape was fitted by the least squares method to obtain the mirror error and rigid body displacement. The surface error contour plots are shown in Fig. 9a and b respectively, and the surface error and rigid body displacement values are shown in Table 1.

4.2. Dynamic analysis

Since the aeronautical optical payload are subjected to aircraft disturbance loads during application, and optical systems are installed inside an inertial stabilized platform, the dynamic performance of the mirror assembly needs to be evaluated. According to
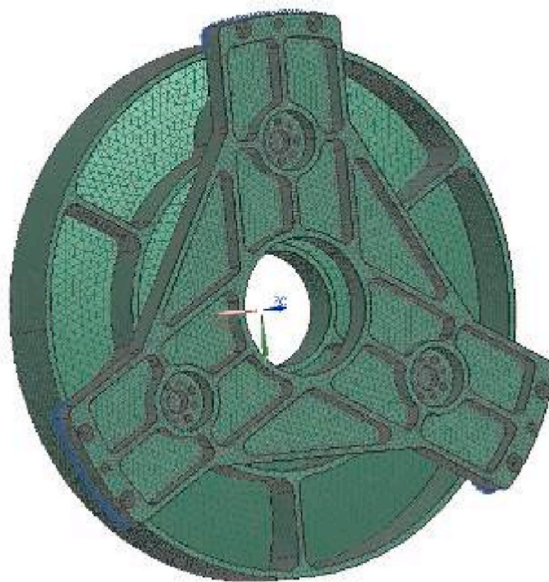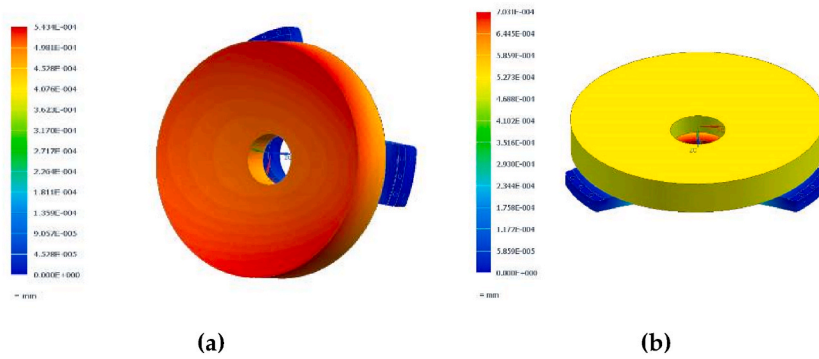

Fig. 7. Diagram of the back plate.

(a)   **(b)**

Fig. 8. Deformation contour plot of the mirror assembly: (a) Under X direction gravity loading; (b) Under Z direction gravity loading.
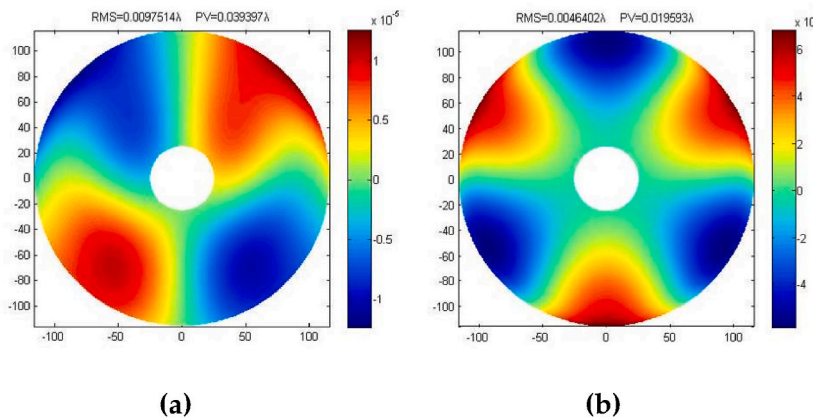

(a)   **(b)**

Fig. 9. Surface error contour plot of the mirror assembly: (a) Under X direction gravity loading; (b) Under Z direction gravity loading.

Table 1
Results of the mirror assembly surface error and rigid body displacement.

Gravity direction	Mirror error (rms)	Displacement	Tilt angle
X	6.17 nm	1.77 μm	1″
Z	2.93 nm	0.48 μm	0″

It can be seen from Table 1 that under the X direction gravity load, the mirror error is 6.17 nm(λ/102), the displacement is 1.77 μm, and the tilt angle is 1''. Under the Z gravity load, the mirror error is 2.93 nm(λ/215), the displacement is 0.48 μm, and the tilt angle is 0''. That meets the system requirements.

the finite element model, the modal analysis method can be used to obtain the modes and mode shapes of the mirror assembly. Fig. 10 shows the mode shape contour of the fundamental frequency of the mirror component, and its fundamental frequency is 672 Hz, which is much higher than the requirement of 150 Hz.

4.3. Temperature analysis

Aviation turrets generally have a temperature control function, which can control the temperature within ±5 °C. The mirror assembly is simulated under both +5 °C temperature increase and −5 °C temperature decrease. The back plate is applied fixed constraints. The surface shape error result is shown in Fig. 11. It can be seen from the figure that under the temperature load of +5 °C and −5 °C, the surface error is 8.6 nm (λ/73). That meets the system requirements.

5. Assembly and results

5.1. Assembly

According to the flexible support structure of the optical mirror designed in this paper, the processing and assembly of a set of
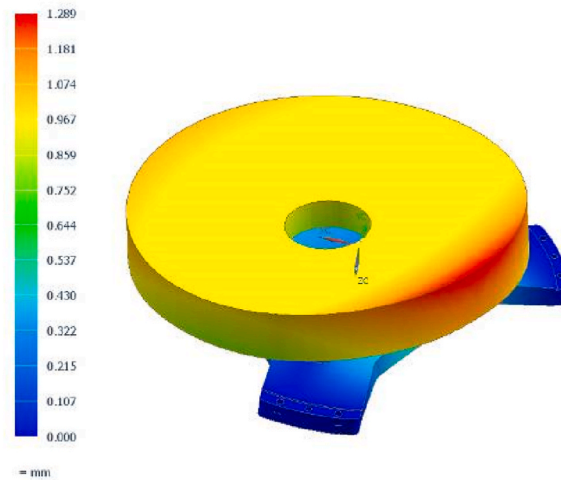
Fig. 10. Fundamental mode shape contour plot of the mirror assembly.
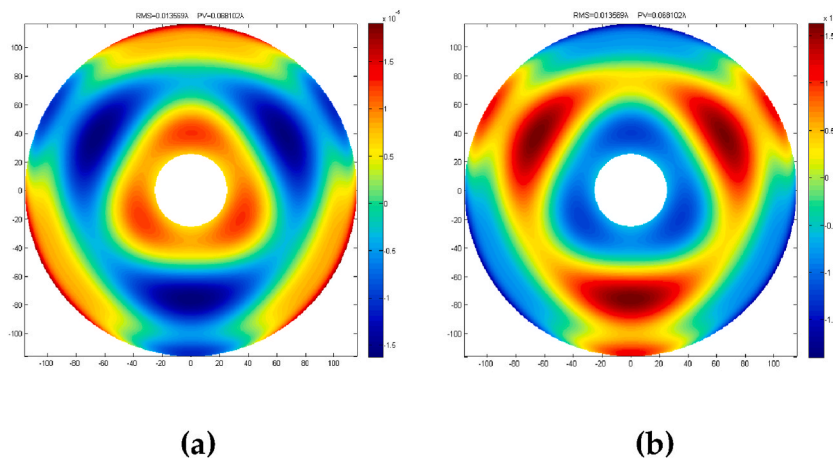

(a)   **(b)**

Fig. 11. Surface error contour plot of the mirror assembly: (a) +5 °C temperature increase; (b) −5 °C temperature decrease.

mirror components was completed. Fig. 12 shows photos of each part of the flexible support mirror structure and the final assembly. Fig. 12a shows a photograph of three adhesive bushings and three composite flexible supports. Fig. 12b shows a photograph of the back plate. Fig. 12c and d are photos of the back and front of the flexible support mirror assembly, respectively.

The adhesive bushings are made of Invar material, which machining method is wire cutting. Its outer circle is ground to fit the mounting holes in the primary mirror.
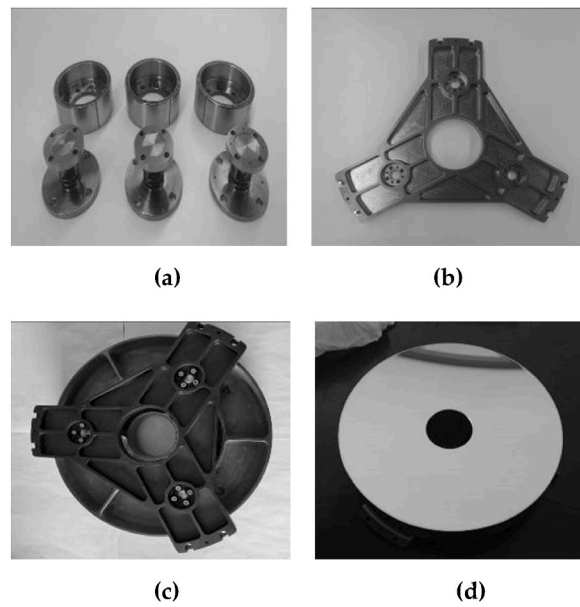
5.2. Results

The mirror error of the flexibly supported mirror assembly was tested in the laboratory using an ZYGO verifier MST 4-inch interferometer, and the test results are shown in Fig. 13. It can be seen from the test results that the surface error value is $\lambda/52$ (rms), which meets the design requirements.

The dynamic performance of the components is tested using platform vibrator, as shown in Fig. 14. A swept sine excitation with an amplitude of 0.2 g and a frequency of 15–2000 Hz was applied in the X axis direction of the mirror assembly. The acceleration response of the mirror was measured, and the fundamental frequency of the final tested mirror assembly was 645 Hz, which was much larger than the 150 Hz required by the design. Compared with the finite element results, the error of simulation analysis is about 4.2%, which basically meets the engineering application.
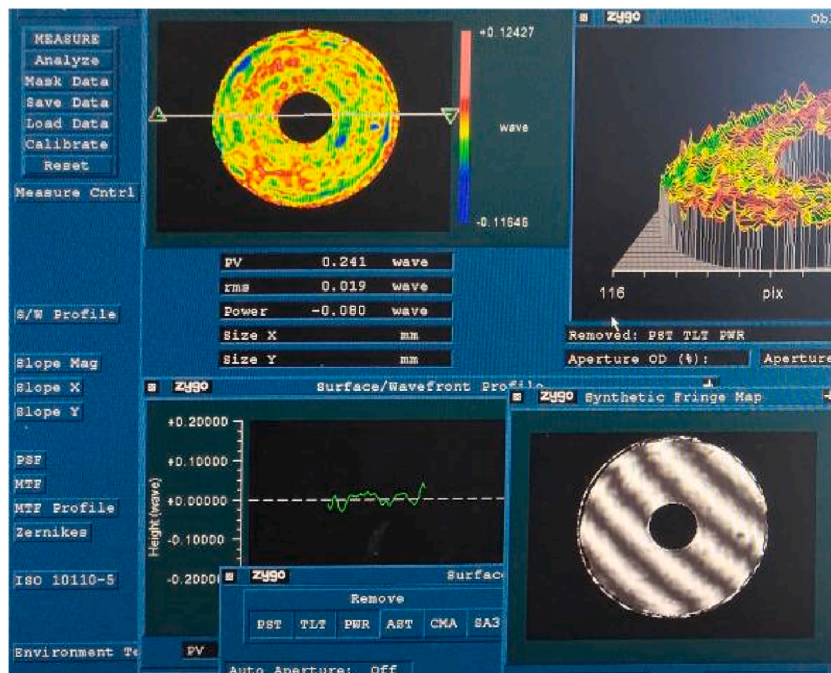
6. Conclusions

In this paper, aiming at the difficult problem of mirror support in aeronautical optical systems, a mirror support structure with

(a) **(b)**

(c) **(d)**

Fig. 12. Photos of components and assembly: (a) Composite flexible supports and adhesive bushings; (b) The back plate; (c) Back of the mirror assembly; (d) Front of the mirror assembly.

Fig. 13. Test results of the surface error of the mirror.

flexible support is proposed. According to the kinematic theory of space mechanism, the spatial degrees of freedom of the mirror are theoretically analyzed. Then, in view of the difficulties encountered in the assembly and application of the mirror, a flexible support structure was designed. Then, the design results are verified by means of finite element analysis. Finally, the processing and assembly of a flexible support structure of the mirror was completed, and the relevant experimental tests were carried out. The experimental results show that the surface accuracy of the mirror after assembly with flexible support structure is better than $\lambda/50$ ($\lambda = 632.8$ nm), the mass is less than 2 kg, and the modal fundamental frequency of the component is 645 Hz. The results meet the requirements for the application of aviation optical systems.

Fig. 14. Dynamics testing of the mirror assembly.

Patents

The research results of this paper have been granted a Chinese invention patent, and the patent number is ZL202010302923.8.

Funding

Author contribution statement

Ning Xu: Conceived and designed the experiments; Performed the experiments; Analyzed and interpreted the data; Wrote the paper.

FuSheng Zhang, AnBo Jiang: Contributed reagents, materials, analysis tools or data.

Data availability statement

Data included in article/supp. material/referenced in article.

Declaration of competing interest

The authors declare that they have no known competing financial interests or personal relationships that could have appeared to influence the work reported in this paper.

References

[1] A. Yavariabdi, H. Kusetogullari, H. Cicek, UAV detection in airborne optic videos using dilated convolutions, J. Opt. 50 (4) (2021) 569–582.

[2] F. Yan, H. Ru, Z. Li, et al., Thickness measurement and three-dimensional structure imaging of oil slick on water by optical coherence tomography, Optik 180 (2018) 1036–1042.

[3] B. Huang, Z.H. Li, X.Z. Tian, et al., Modeling and correction of pointing error of space-borne optical imager, Optik 247 (2021), 167998.

[4] D. Schedl, I. Kurmi, O. Bimber, Search and rescue with airborne optical sectioning, Nat. Mach. Intell. 2 (12) (2020) 783–790.

[5] W.M. Zhang, B. Wang, Y.Q. Li, et al., Underwater image enhancement combining dual color space and contrast learning, Optik 247 (2023), 170926.

[6] F. Xue, W. Jin, S. Qiu, J. Yang, Airborne optical polarization imaging for observation of submarine Kelvin wakes on the sea surface: imaging chain and simulation, ISPRS J. Photogrammetry Remote Sens. 178 (2021) 136–154.

[7] M.A. Rania, M.A.A. Mahmoud, A. Mostafa, Characterization of thick and contact lenses using an adaptive Shack–Hartmann wavefront sensor: limitations and solutions, Optik 283 (2023), 170922.

[8] M. Zhang, Q. Lu, H. Tian, D. Wang, C. Chen, X. Wang, Design and optimization for mounting primary mirror with reduced sensitivity to temperature change in an aerial optoelectronic sensor, Sensors 21 (2021) 7993.

[9] H. Li, H. Zhang, Y. Ding, J. Zhang, Y. Cai, Contributions of support point number to mirror assembly thermal sensitivity control, Sensors 23 (2023) 1951.

[10] C. Li, Y. Ding, C. Lin, Y. Wei, Y. Zheng, L. Zhang, Optomechanical design and simulation of a cryogenic infrared spectrometer, Appl. Opt. 59 (2020) 4642–4649.

[11] T. Chen, Y. Wu, Design and alignment of airborne compact long focal length optical system, Acta Photonica Sin. 50 (11) (2021) 204–214.

[12] M. Shao, L. Zhang, X. Jia, Optomechanical integrated optimization of a lightweight mirror for space cameras, Appl. Opt. 60 (2021) 539–546.

[13] K. Wang, J. J, Dong, P. Zhou, X. Wang, P. Jiang, Back support structure design of mirror of space remote sensor, Infrared Laser Eng. 48 (7) (2019) 11.

[14] H. Kihm, H.S. Yang, K. Moon, J. Yeon, H.S. Lee, Y. Lee, Adjustable bipod flexure for mounting mirrors in a space telescope, Appl. Opt. 51 (2012) 7776–7783.

[15] B. Liu, W. Wang, Y.J. Qu, X.P. Li, X. Wang, H. Zhao, Design of an adjustable bipod flexure for a large-aperture mirror of a space telescope, Appl. Opt. 57 (2018) 4048–4055.

[16] P. Zhou, D. Zhang, G. Liu, C. Yan, Development of space active optics for a whiffletree supported mirror, Appl. Opt. 58 (2019) 5740–5747.

[17] L. Zhang, T. Wang, F. Zhang, H. Zhao, Y. Zhao, X. Zheng, Design and optimization of integrated flexure mounts for unloading lateral gravity of a lightweight mirror for space application, Appl. Opt. 60 (2021) 417–426.

[18] P. Jiang, P. Zhou, Optimization of a lightweight mirror with reduced sensitivity to the mount location, Appl. Opt. 59 (2020) 3799–3805.

[19] R. Hu, S. Liu, Q. Li, Topology-optimization-based design method of flexures for mounting the primary mirror of a large-aperture space telescope, Appl. Opt. 56 (2017) 4551–4560.

[20] P. Zhou, S. Xu, C. Yan, X. Zhang, Research on neutral surface of lightweight, horizontally supported mirror, Opt. Eng. 57 (2018), 025107.